INL/CON-13-28860
PREPRINT

A Novel Laser-Based Approach for Cleaning Contaminated Metallic Surfaces Coupled with Rapid Residue Analysis

SPIE-DSS 2013

Robert V. Fox
Lauren Roberts
Frank C. DeLucia, Jr.
Andrzej W. Miziolek
Andrew I. Whitehouse

May 2013

The INL is a
U.S. Department of Energy
National Laboratory
operated by
Battelle Energy Alliance

A novel laser-based approach for cleaning contaminated metallic surfaces coupled with rapid residue analysis

Robert V. Fox*, Lauren Roberts
Idaho National Laboratory, Idaho Falls, ID, 83415

Frank C. DeLucia, Jr. and Andrzej W. Miziolek
US Army Research Laboratory, Aberdeen Proving Ground, MD, 21005

Andrew I. Whitehouse
Applied Photonics Ltd, Skipton, North Yorkshire, BD23 2DE, UK

ABSTRACT

We are developing a novel approach for cleaning and confirming contaminated metallic surfaces that is based on laser ablation to clean the surfaces followed closely in time and space by laser analysis of the degree of cleanliness. Laser-based surface cleaning is a well-established technology and is commercially available (e.g., Adapt-Laser). The new development involves the integration of a LIBS (Laser Induced Breakdown Spectroscopy) surface analytical capability to analyze the surface before and right after the laser cleaning step for the presence or absence of unwanted residues. This all-laser approach is being applied to surfaces of steel vessels that have been used for the containment and destruction of chemical munitions. Various processes used for the destruction of chemical munitions result in the creation of oxidized steel surfaces containing residues (e.g., arsenic, mercury) that need to be removed to acceptable levels. In many instances inorganic molecular contaminants become integrated into oxide layers, necessitating complete removal of the oxide layer to achieve ideal levels of surface cleanliness. The focus of this study is on oxidized steel surfaces exposed to thermally decomposed Lewisite, and thus laden with arsenic. We demonstrate here that a commercially-available cleaning laser sufficiently removes the oxide coating and the targeted contaminants from the affected steel surface. Additionally, we demonstrate that LIBS is useful for the identification of arsenic and mercury on steel surfaces before and after laser cleaning, with arsenic being specifically tracked and analyzed at levels less than 1 microgram per square centimeter surface loading. Recent progress and future directions are presented and discussed.

Keywords: laser-induced breakdown spectroscopy (LIBS), laser cleaning, contaminated surface analysis, chemical munitions, arsenic.

1. INTRODUCTION

Laser mediated surface cleaning has been demonstrated for various applications ranging from removal of contaminant particles on the surfaces of silicon wafers (microelectronics industry), to removal of oxides and encrustations found on artwork and artifacts (conservation and restoration industries) [1 - 17]. Recent reports have shown the utility of laser cleaning for paint stripping, radioactive decontamination, removal of surface greases/oils, and decontamination of surfaces exposed to chemical weapons agents. The extent to which a surface is "cleaned" by laser treatment has been assessed by a variety of analytical techniques including acoustic spectroscopy, diffuse/specular reflectance spectroscopy, scanning electron microscopy, infrared spectroscopy, Raman spectroscopy, x-ray fluorescence spectroscopy, secondary ion mass spectrometry, and gamma ray spectroscopy, just to name a few [18 - 20]. In those cases where the speed, sensitivity, and cost of the surface analysis technique are critical to the "success" of the cleaning operation, the choice of which surface analysis tool to use becomes as important as the laser cleaning function.

The US Army Office of the Project Manager for Non-Stockpile Chemical Materiel (PM – NSCM) has recently investigated laser cleaning in the re-deployment lifecycle for removal of inorganic chemical warfare materiel (CWM) residues from steel surfaces and steel parts.

*robert.fox@inl.gov; phone 208-526-7844; fax 208-526-8541

Next-Generation Spectroscopic Technologies VI, edited by Mark A. Druy, Richard A. Crocombe, Proc. of SPIE Vol. 8726, 87260N

The laser cleaning technology was recently tested on Explosive Destruction System (EDS) parts which had seen service destroying CWM, including some arsenical rounds. Results from that investigation demonstrated that knowledge of surface inorganic contaminant species that are present, their concentration ($\mu g/cm^2$), and their spatial distribution is vital for assessing the effectiveness of a laser surface cleaning effort [21]. Further, it was observed that a more powerful, real-time surface analytical tool would add considerable value to surface cleaning operations by allowing for contaminant identification, concentration, and location on the surface to be determined before and after laser cleaning. When operated in an ideal mode, the time span between surface analysis and laser cleaning would either be real-time, or near-real-time to allow for the analytical feedback to direct the laser cleaning function.

In this study we assess the utility of laser cleaning for the removal of arsenic and mercury from heavily oxidized ton container eductor tube surfaces. We employ a commercially-available Nd:YAG laser operating at approximately 28 kHz to bring about removal of the oxide layer on steel surfaces, and the molecular contaminants that have penetrated and become integral to the oxide layer. We also demonstrate the utility of a field-portable Laser Induced Breakdown Spectrometer (LIBS) to detect contaminants of interest before and after laser cleaning cycles. We utilize the near-real-time analytical output from the LIBS to guide surface cleaning decisions while the cleaning is in progress.

2. EXPERIMENTAL

2.1 Test subjects: contaminated ton container eductor tubes.

The US Army PM – NSCM has the mission responsibility for the destruction and disposal of all applicable CWM in a safe and environmentally acceptable manner. In the process of accomplishing that mission, NSCM has become the steward of various pieces of contaminated equipment, containers, and steel surfaces that must be frequently decontaminated and cleaned between deployments. The acts of: a) cleaning the equipment, b) assessing its cleanliness level, and c) clearing equipment for re-deployment are essential components of the re-deployment lifecycle of usable equipment and containers. The Army also possesses facilities and equipment that are no longer serviceable, or have reached the end of their service life. Those facilities and pieces of equipment are decontaminated and decommissioned. In the case of steel surfaces and equipment, many of the decommissioned materials that have been decontaminated still contain inorganic CWM residues (e.g., mercury, arsenic, etc) that are a direct result of the CWM decontamination process, and have not been removed by the CWM decontamination process. Atomic and molecular contaminant species become integrated into oxide layers as the steel surface oxidizes. Thermal decontamination processes can destroy active CWM agents, but give rise to atomic residues which can penetrate oxide layers. For this study we have selected heavily oxidized chemical ton container eductor tubes laden with CWM residues left over from thermal decontamination processing (i.e., the 5X process).

Ton containers are carbon steel (carbon content <0.31% as designated in 49 CFR 173.300), cylindrical containers equivalent in length and diameter to two stacked 55-gallon drums (Figure 1). A ton container weighs approximately 1,600 pounds empty and measures nearly seven feet in length, and approximately 30 inches in diameter. The US Army has used ton containers to store and ship bulk chemicals, including chemical agent, since the 1930s. Ton containers are equipped with eductor tubes for removal of liquid-phase materials (see (B) Valve Agent in Figure 1). Eductor tubes are approximately 14 - 18 inches in length and 1.375 inches in diameter with an elongated S-curvature (Figure 2). Thermal decontamination of ton containers includes draining liquids from the container and then heating the entire container to a temperature >583°C (1000°F) for >15 minutes; that process constitutes what is called the "5X" level of decontamination. Containers are then cut apart and the metal is sold for scrap.

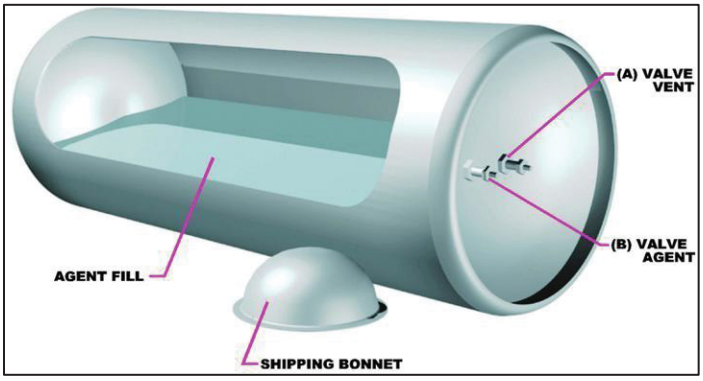

Figure 1. Cross-Section of Chemical Ton Container.
(photo courtesy of the US Army Chemical Materiel Activity).

The Idaho National Laboratory (INL) obtained approximately 20 ton container eductor tubes which had undergone the 5X decontamination process. The service history and origin of each tube is unknown. Tubes arrived in a single shipping container and were not segregated, leading to cross-contamination throughout the entire tube population that was received. Eductor tubes were clamped into a vise, and cut with a reciprocating saw into smaller

pieces (~4.5" – 5" long) for use in the laser cleaning tests (Figure 3). Eductor tubes contained significant surface corrosion products and deposits of inorganic CWM residues arising from naturally occurring oxidation of the carbon steel container, and from thermally-induced oxidation of CWM during the decontamination process (Figures 4 and 5). In some instances agglomerated Hg droplets have been observed associated with the oxide from the inside of the ton container. Exfoliation of container oxide layers and thermal decomposition products lead to rust and other solid encrustations found on the eductor tube. Selected inorganic contaminants of interest found on 5X eductor tubes included As, Hg, Fe, Mn, Ni, Cr, P, S, Zn, Pb and Cd. Table 1 below gives atomic composition information for the rust that was obtained from a composite grab sample of eductor tube rust. The data were obtained via digestion of the rust and examination of atomic species by Inductively Coupled Plasma Mass Spectrometry (ICP-MS), and Optical Emission Spectrometry (ICP-OES).

Figure 2. Eductor tube from a chemical ton container.

Figure 3. Sectioned piece of eductor tube.

Figure 4. Solids from inside a thermally treated ton container (photo courtesy of Shaw Environmental).

Figure 5. Texture of oxide coating on an eductor tube.

Table 1. ICP-MS, ICP-OES Results for Selected Eductor Tube Samples

	Eductor Tube Rust		Eductor Tube Basis Metal	
Analyte	Conc. µg/g	Conc. Wt%	Conc. µg/g	Conc. Wt%
Phosphorus	183.50	0.0184	4644.74	0.46
Chrome	145.53	0.0146	86.39	0.0086
Manganese	2335.75	0.23	2729.28	0.27
Nickel	265.21	0.0265	37.11	0.0037
Cadmium	0.61	6.08E-05	BDL	BDL
Lead	303.50	0.0304	BDL	BDL
Arsenic	170696.51	17.07	35.85	0.0036
Mercury	8690.92	0.87	BDL	BDL
Iron	481900	48.19	984700	98.47
Zinc	BDL	BDL	2.06	2.06E-04
Sulfur	1140	0.11	14.43	0.0014

*BDL = below method detection limit.

Data found in Table 1 show that very little arsenic may be found as an inherent contaminant in the basis metal. Arsenic primarily arises as an inorganic contaminant left over from thermal decomposition of arsenical chemical agents (e.g., Lewisite). Lead, cadmium, mercury, sulfur, nickel and chrome can also be found in the rust at higher concentrations than in the basis metal. Of those contaminants arsenic was quantitatively tracked in this study, and mercury was qualitatively tracked by simply noting its absence or presence in the acquired LIBS spectra. Arsenic chemical speciation, concentration, oxidation state, spatial distribution, and depth of penetration into the eductor tube oxide layer have been studied and reported [22].

2.2 Laser Induced Breakdown (LIBS) Spectrometer.

Laser induced breakdown spectroscopy (LIBS) is an atomic-emission spectroscopy technique that uses a focused laser pulse of sufficient energy to ablate a small amount of the target sample and generate a microplasma, which is typically around 15,000 K, and is visible to the eye as a flash of white light. Light emission from the atomized and excited target material is generated in the process of relaxing back to the ground state. Emitted photons are characteristic of the elemental composition of the surface solids, i.e., the intensity at a given wavelength tracks the concentration of the element while the specific wavelength of the captured light is unique to each element, so that once the wavelength is measured then the responsible element is known from NIST spectral databases. Emitted photons are captured and separated based on wavelength using a dispersive spectrometer. The intensity of the emissions at various wavelengths are detected and quantified using a detector, i.e., a photomultiplier tube (PMT) or a charged couple device (CCD). A schematic of how LIBS spectra are acquired is found in Figure 6. The advantages of LIBS include (1) speed of analysis (real-time), (2) sensitivity, (3) specificity, and (4) a full elemental inventory of the sample is capture in each laser shot when using a broadband, high resolution spectrometer.

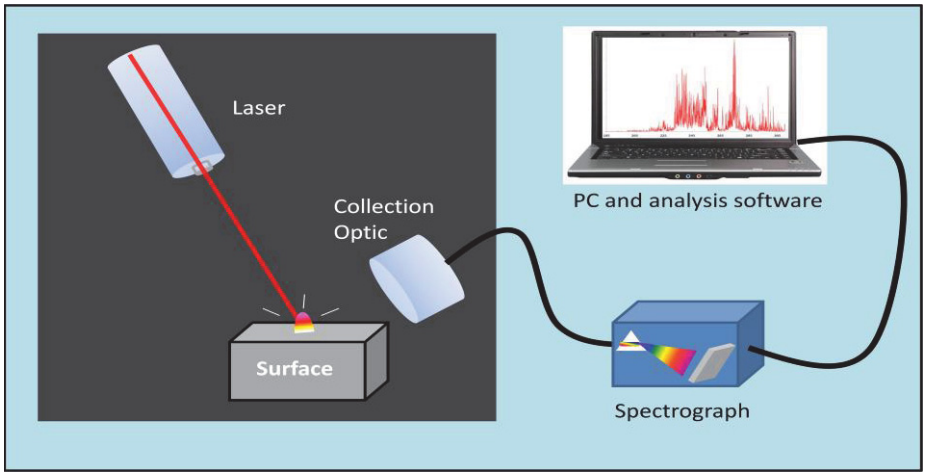

Figure 6. Diagram of how LIBS spectra are acquired. A laser is focused onto a surface to be analyzed. Light emitted from the resulting surface plasma is collected and transferred to a spectrograph where photons are separated by wavelength. Photon intensity at any given wavelength is measured by a detector. Signal from the detector is displayed on a PC.

LIBS spectrometers used for analysis were provided by the Army Research Laboratory (ARL) and were manufactured by Applied Photonics (AP) (Applied Photonics Ltd., Skipton, UK). The LIBSCAN 100 (Figure 7) uses a focused Nd:YAG laser (~100 mJ/pulse@1064 nm) to produce surface plasma. Emitted light is captured and sent to a Czerny-Turner spectrograph (Avantes BV, Apeldoorn, The Netherlands). The intensity of resolved photons is quantified using a CCD array, and signal from the CCD array is sent to a personal computer (PC) equipped with spectral analysis software. The LIBSCAN 100 was used in conjunction with a modular sample chamber (Figure 8) which allowed flooding of the sample and chamber with argon gas, and allowed mounting of the LIBS unit at a set focal distance away from the surface of the sample to be analyzed. A manual sample stage allowed *x-y-z* movement of the sample to different sampling locations, and refinement of the focal distance. Signal from the spectrograph and CCD array was visually displayed on a laptop PC allowing for on-the-spot viewing and manipulation of the spectra. Spectrometers were calibrated using standardized coupons developed at the INL.

Selected eductor tube pieces were analyzed via LIBS before laser cleaning, were laser cleaned one time, and then analyzed via LIBS after laser cleaning. If the LIBS analyzer showed no surface contaminant after the first laser cleaning cycle, then the test piece was removed from the cleaning tests. If LIBS analysis showed arsenic remaining on the eductor tube then the test piece was returned for a second round of laser cleaning. The "clean" and then "analyze" process was repeated until arsenic was below LIBS instrument detection levels.

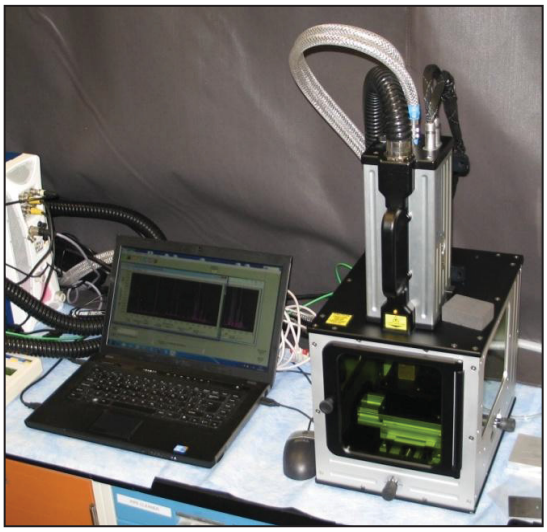

Figure 7. LIBSCAN 100 mounted on top of a modular sample chamber.

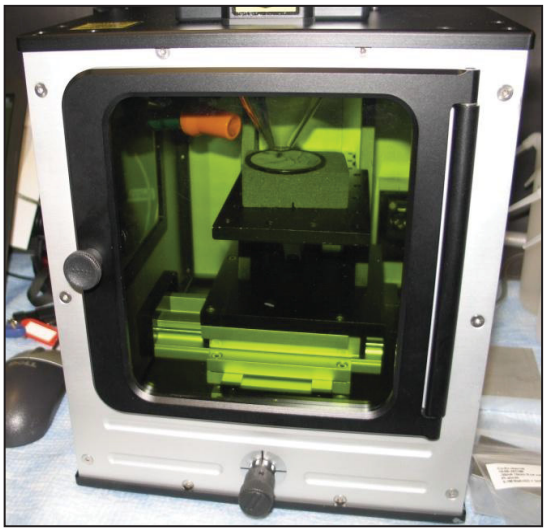

Figure 8. Modular sample chamber with x-*y*-*z* sample positioning stage.

2.3 Calibration of the LIBS spectrometer for quantitative measurement of arsenic.

LIBS spectra provide photon intensity and wavelength of the emissions captured. To convert photon intensity to a corresponding analyte concentration, surfaces having known amounts of analyte per unit area were needed to construct a calibration curve for the LIBS spectrometer. There are numerous different ways to make standardized surfaces. Since the LIBS laser samples such a small area, ~0.008 cm^2 per shot, then analytes of interest need to be microscopically homogeneous in their dispersal over the surface, and need to be affixed in a manner that allows easy access by the LIBS laser without fear of the analyte being removed through incidental contact between the surface and a gloved hand or specimen bag. To further complicate the issue of making a set of standardized coupons, such factors as surface physical heterogeneity (i.e., cracks, pits, etc) needed to be addressed, as well as problems associated with surface tension, adhesion of liquid spikes, matrix composition (pre-existing contaminant inherent to the basis material), and matrix affects on analyte signal. Arsenic chemistry is also complex and oxidation state, speciation, and chemical stability need to be considered. For standardized coupons we chose both chemical plating and electroplating techniques after much research, and trial and error. Blank carbon steel coupons were measured (length and width dimensions to the nearest 0.1 mm), cleaned with soap and water, allowed to dry, and then were polished to a level of 1000-grit to remove gross surface features such as scratches, pits, and cracks. Polished coupons were cleaned again with soap and water and triple rinsed in nanopure water. Dried coupons were then washed in solvents to remove any oils, lingering organic contaminants, and polishing waxes. Cleaned coupons were marked on their backsides with an identification number, and the backsides were then masked using clear plastic packaging tape.

Cleaned, marked, and masked carbon steel coupons were dipped for 10 seconds into a chemical solution comprised of 50 mM copper sulfate and 1 molar sulfuric acid. This technique caused for chemical plating of a thin film (several monolayers) of metallic copper onto the surface of the steel coupon, filling voids and providing a more uniform chemical surface upon which arsenic could then be alloyed. Coupons were removed from the plating solution, rinsed with nanopure water, and then dried using forced hot air. Dried coupons were then dipped for 10 seconds into a second plating solution containing arsenous acid (sodium salt), 50 mM copper sulfate, and 1 molar sulfuric acid.

Arsenic is known to alloy easily with copper and iron. In the second dip solution arsenic and copper in solution are chemically plated (reduced) onto the surface of the thin film of copper over carbon steel. The technique is known throughout metal plating operations and creates a thin, strongly-adhering film of alloyed copper-arsenic. Varying the concentration of arsenic in the second dip solution, and the length of the dip time, will result in thin films having different concentrations of arsenic per unit area dispersed in a very homogeneous manner throughout the copper film. Film thickness was found to be uniform and on the order of 1 – 10 microns depending on immersion time. A single shot from the LIBS laser was found to completely penetrate the copper-arsenic layer and proceed on into the substrate. Coupons having arsenic coverage ranging from ~0.06 to ~16.8 μg/cm^2 were made. Blanks comprised of copper over carbon steel were also made.

To determine and confirm arsenic concentration on the surfaces of the standardized coupons three identical coupons of each series, including blanks, were selected and digested in 30% aqua regia. After digesting for ~75 minutes the entire film of copper plating was digested and the aqua regia began to etch the carbon steel substrate. After ~75 minutes the digestion was halted by removing the coupon from the digest solution, rinsing the coupon with nanopure water, and combining the rinsate and etchate (which collectively shall be called the etchate) into a single volumetric flask for standardized dilution. The diluted etchate was filtered through a 0.45 μm hydrophilic Teflon filter, and a portion was given for ICP-MS analysis. Additionally, standardized coupons that had been chemically plated were analyzed using Imaging Time of Flight Secondary Ion Mass Spectrometry (ToF-SIMS) to confirm the chemical microscopic homogeneity imparted by the plating technique. In this manner standardized coupons were made and characterized, surface chemical homogeneity was examined, uniform arsenic loadings were confirmed, and series of coupons spanning arsenic surface loadings from ~0.06 to ~16.8 μg/cm^2 were made to calibrate the LIBS spectrometers.

LIBS spectrometers were calibrated by acquiring multiple shots from each of the different calibration coupons. All LIBS spectra were converted from ASCII x – y text files (variable x-spacing) to GRAMS/AI v9.1 (Thermo Fisher Scientific, Waltham, MA) files using the GRAMS/AI converter. Using GRAMS/AI, spectral limits were truncated to 313 nm, spectra were baseline corrected, and normalized to a predominant ubiquitous atomic line (e.g., iron, argon, etc). Arsenic peaks at ~197.1 nm, and ~228.8 nm were used for examining spectral statistics, and for generation of standard curves. Several different peak analysis techniques were employed (e.g., peak height, integrated area); each technique providing similar results. In the case of carbon steel coupons and eductor tubes, both arsenic peaks at ~197.1 nm and ~228.8 nm could be used for determining the concentration of arsenic on the test piece.

To examine spectral statistics and relative standard deviation associated with the calibration sets, five different spectra, each a composite of 25 spectra, were collected for each coupon. A mean, and a standard deviation (SD) of the population from the mean, were calculated for the ~228.8 nm arsenic peak from the 5 composite spectra for each coupon. Percent relative standard deviation (RSD%) was calculated as (100*SD)/mean. The Limit of Detection (LoD) for the equipment used under the given test conditions was calculated as three times the standard deviation at zero arsenic concentration (blanks) divided by the slope of the calibration curve through the data at zero concentration arsenic (blanks).

2.4 Commercial laser cleaner and laser cleaning of test pieces.

Figure 9. Commercial 500 Watt cleaning laser from Adapt-Laser (Kansas City, MO).

Figure 10. Terminal optic of the cleaning laser.

A 500 watt commercial-grade Nd:YAG laser from Adapt-Laser (Kansas City, MO) (Figure 9) was used for cleaning test pieces. The laser operates at a user-variable repetition rate (~10 – 50 kHz). Laser light entering the terminal optic (Figure 10) via fiber optic bundle strikes a galvanometer-driven mirror cycling at a rate of approximately 100 Hz. The mirror rasters the laser beam horizontally left-to-right to create a "line of light" 2" – 3" wide, with a focal point approximately 130 mm from the end of the exit window. The line of light created by the rastered beam results in creation of a surface plasma that photothermally vaporizes materials from the surface that absorb 1064 nm light.

A Class-A chemical fume hood at the INL Research Center laboratory A-17 was prepared by installation of a laser curtain around the perimeter of the hood. The curtain enclosed an area ~12' wide by ~16' long in front of the hood, which became the laser control area for these studies. Access to the control area was manually controlled by the laser operator and an INL staff member stationed outside the control area while the laser was in operation. Entry/exit to the area was accomplished by a Velcro-sealed sash in the laser curtain. The INL Laser Safety Officer designated the entire area within the control area as the nominal hazard zone. The LIBS spectrometers were co-located in the laser control area although they were operated in a Class I configuration.

Laser cleaning of test pieces was performed inside of the fume hood. The end-effector of the cleaning laser was positioned inside of the fume hood along with a 6 hp HEPA-filtered ShopVac that was used to draw off particulates and fumes generated during ablation of contaminants. The vacuum intake was located proximal to the where the laser generated the plasma plume. The location of the vacuum intake was modified several times during the tests to achieve optimal performance. The laser power supply and cooling unit were positioned outside of the control area near the front of the lab. A 50 ft fiber-optic cable attached the end-effector to the laser power supply. The laser shutter was controlled by a dual-stop trigger on the end-effector, and the laser operator had control over the shutter during laser operations.

A pre-operation walk down was performed by INL facilities and safety staff prior to laser operations. All safety measures and hazard controls were inspected and tested including hood operation/certification, laser testing and inspection, and inspection of PPE and laser safety glasses. An INL Industrial Hygienist affixed an air sampling/monitoring device to the outside of the hood face, directly above the sash, and the device collected air samples during laser cleaning of test pieces. Rotary stages were positioned in the fume hood where test pieces could be placed and rotated while being cleaned, without having to touch the test piece.

Prepared eductor tube test pieces were weighed, analyzed via LIBS, and then transferred to the fume hood for laser cleaning. The laser operator cleaned test pieces at a laser power that left test pieces clean upon visual inspection. The amount of time the laser operator spent on each piece was left to the discretion of the operator, but typically was ~ 5 minutes total per test piece (~2.5 minutes each side). The focal distance of the laser was ~ 130 mm; however, it was reported by the laser manufacturer and confirmed by the laser operator that the focal point "sweet spot" had about $\pm$ 2 cm of "play". The "sweet spot" was found by aiming the end effector at the test piece, engaging the dual-stop trigger, and then using visual and audible sensory input to achieve the greatest plasma intensity and cleaning affect. Once the proper focal distance was found, the operator would sweep the end-effector back and forth over the part and visually observe cleaning. Visual inspection of cleaning was easily accomplished while wearing suitable laser safety glasses, which were always worn while lasers were in operation. Using a clean glove, the operator would turn the rotary stage upon which the part sat in order to achieve cleaning from all sides. Using a clean glove, the operator was able to turn the part over and achieve cleaning of the opposite side of each test piece as necessary. Figure 10 above shows the laser operator performing a cleaning operation.

3. RESULTS AND DISCUSSION

3.1 Calibration of the LIBS spectrometer for arsenic.

The calibration curves for the ~197.1 nm and ~228.8 nm arsenic peaks are shown in Figures 11 and 12, respectively. Statistical treatment of each series of five spectra collected from each standard coupon was performed for the ratio ~228.8 nm arsenic peak area to the ~229.4 nm peak area. Relative standard error measured across all arsenic calibration sets averaged 5.6 $\pm$ 2.1 (RSD %). A second-order polynomial fit of the ~228.8 nm arsenic calibration data provided a Limit of Detection (LoD) of 0.23 µg/cm^2 arsenic loading, and an R^2 = 0.95; however, a second examination of the ~228.8 nm spectral data yielded a LoD of 0.19 µg/cm^2 (3*0.0060/0.0941) with an R^2 = 0.98 by using a power function trend line, which proved to be a better fit to both sets of data. The Limit of Quantitation (LoQ) was established as 0.57 µg/cm^2 arsenic loading.

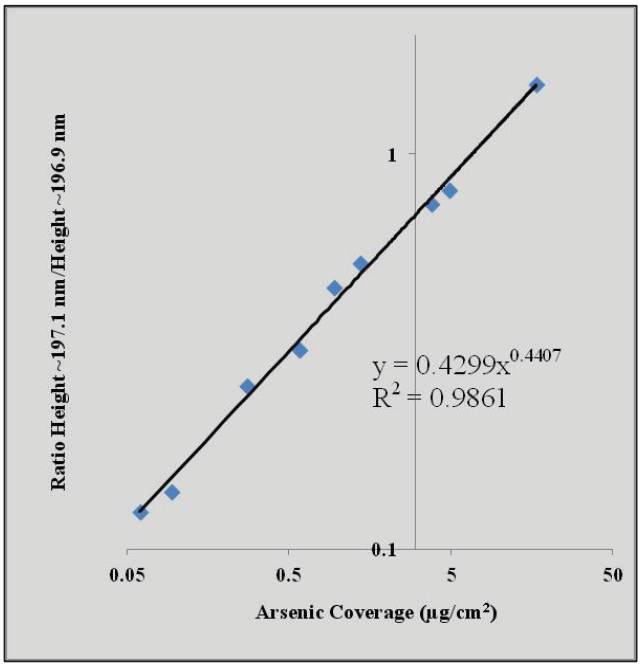

Figure 11. LIBS calibration curve for the 197.1 nm peak. The data in the plot show the ratio of the height of the 197.1 nm peak to the 196.9 nm peak.

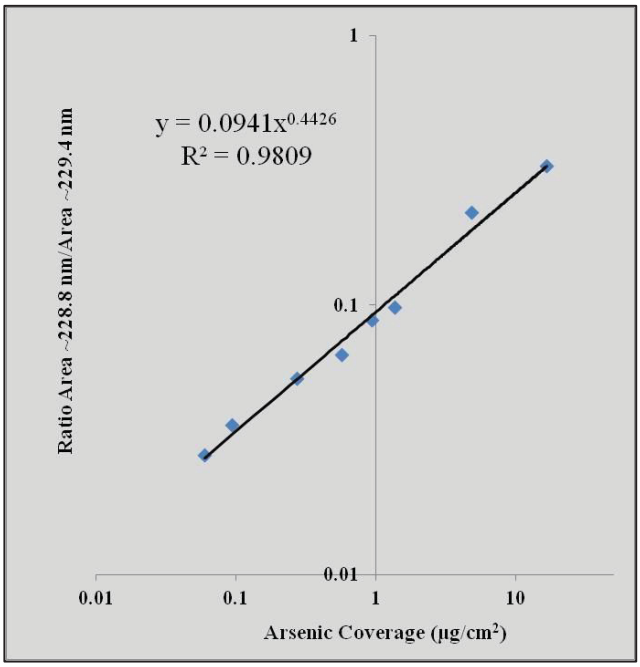

Figure 12. LIBS calibration curve for the 228.8 nm peak. The data in the plot show the ratio of the area of the 228.8 nm peak to the 229.4 nm peak.

3.2 Qualitative analysis of mercury using LIBS.

From previous work mercury was found to be a contaminant of interest; appearing both on the surface and within the oxide layers found on the eductor tubes [22]. In some instance intact drops of mercury were noted associated with the eductor tube rust, but the ICP-MS data indicated mercury appearing at an average value of ~ 0.87 wt% in the composite rust grab sample. Although mercury was not quantitatively tracked in this study the LIBS spectrometer collected plasma emission light in the wavelength range of ~200 nm to ~900 nm. Mercury has a predominant atomic emission line appearing at approximately 435.8 nm which does not overlap any other basis metal atomic line. Thus, for qualitative purposes, the ~435.8 nm peak could be tracked on eductor tube samples before and after laser cleaning to determine what affect laser cleaning was having on mercury associated with the oxide layer.

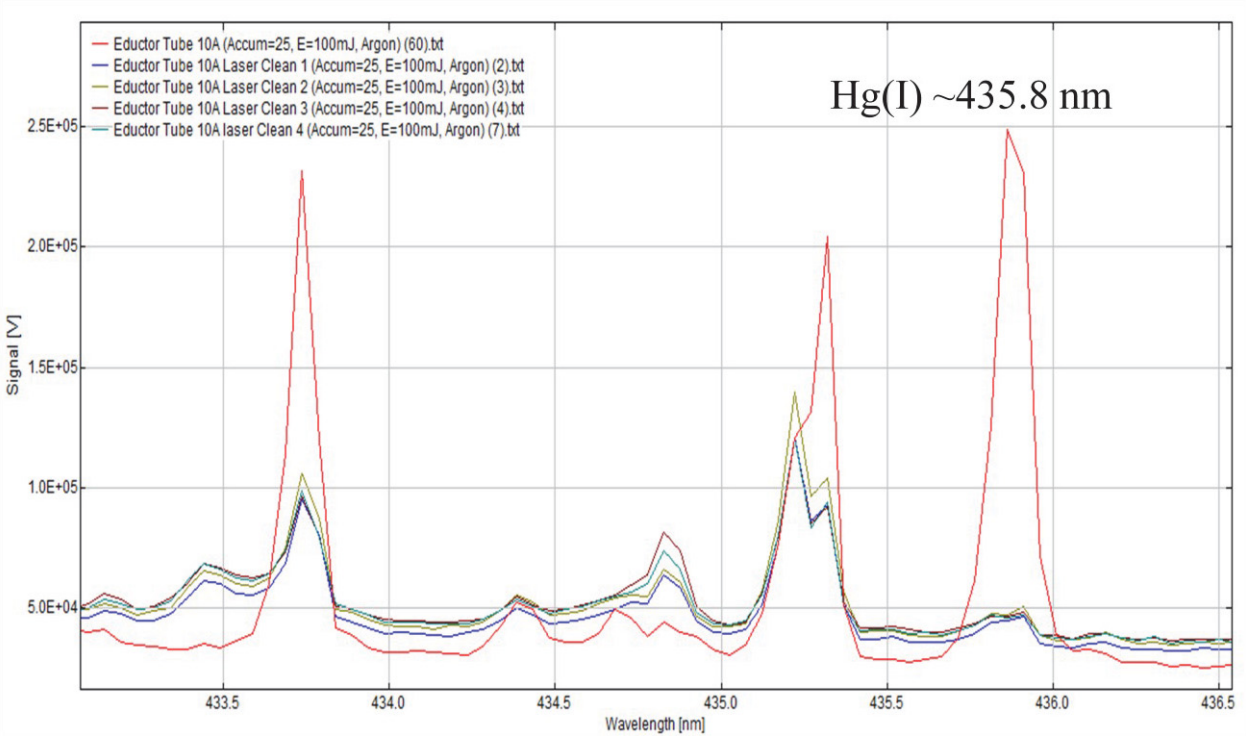

Figure 13. Screen shot from the LIBS spectral analysis software during laser cleaning and LIBS analysis of eductor tube sample ET-10A. The mercury line at ~435.8 nm disappears to background levels after the first laser cleaning round.

A screen shot from the LIBS spectral analysis software is given in Figure 13 above. The red line shows abundant mercury signal appearing at ~435.8 nm on the eductor tube piece (ET-10A) before laser cleaning. After the first round of laser cleaning the mercury signal drops to background levels typically found on clean carbon steel. The ~435.8 nm line was monitored for each eductor tube piece before and after laser cleaning. It was found, for all pieces, that mercury was effectively removed in the first laser cleaning round.

3.3 Arsenic analysis via LIBS and laser cleaning of eductor tubes.

Fourteen separate pieces of eductor tube were analyzed via LIBS, and then laser cleaned. The primary data that indicate success of these tests is arsenic associated with the eductor tubes before and after laser cleaning. Table 2 shows the concentration of arsenic found on each eductor tube test piece before and after laser cleaning as measured by LIBS.

Table 2. Eductor Tube Arsenic Concentrations Before and After Laser Cleaning As Determined By LIBS.

	LIBS Before	LIBS After	Cleaning
Sample	Arsenic (μg/cm^2)	Arsenic (μg/cm^2)	Cycles
ET-1A	~0.56	BDL	1
ET-1B	0.82	BDL	1
ET-2A	0.94	BDL	1
ET-2B	1.05	BDL	1
ET-4A	0.99	BDL	1
ET-4B	3.25	BDL	1
ET-5A	6.69	BDL	1
ET-5B	1.89	BDL	1
ET-6B	6.16	BDL	2
ET-10A	8.86	BDL	4
ET-10B	7.39	BDL	3
ET-11A	1.47	BDL	1
ET-13B	5.03	BDL	2
ET-14B	3.03	BDL	2

From Table 2 it is seen that arsenic concentrations are measurable on the eductor tube test pieces before laser cleaning. In some cases there is as much as 7X to 8X the US Army administrative control level of arsenic (1 μg/cm^2). LIBS analysis of eductor tube surfaces after the final round of laser cleaning shows arsenic values below the LIBS detection limit of 0.23 μg/cm^2 (BDL = Below

Detection Limit in Table 2). From Table 2 it is also seen that while many test pieces required a single cleaning round, at least 5 different pieces required more than one round of laser cleaning. In those cases the LIBS demonstrated arsenic was still present on the test piece after the initial cleaning round. When that occurred the test piece was returned to the hood and cleaned again. After a second cycle of laser cleaning the test piece was removed and re-analyzed via LIBS. Laser cleaning/LIBS analysis cycles were repeated until the test piece was cleaned to below detection limits.

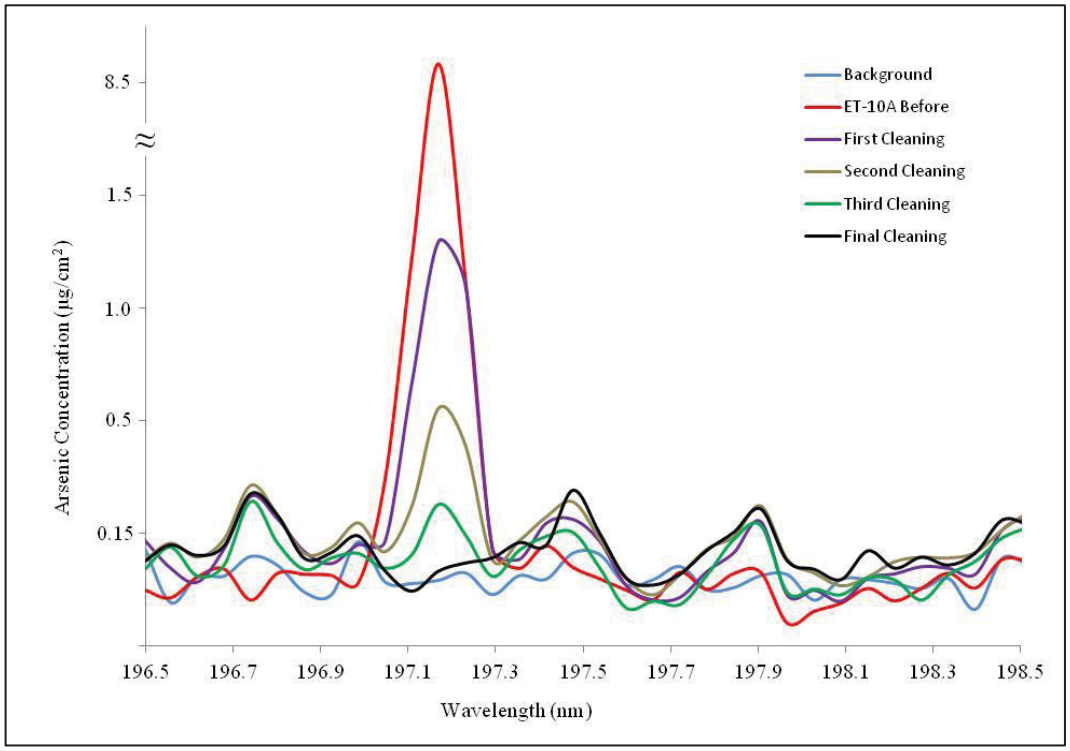

Figure 14. Plot of LIBS signal from ET-10A before laser cleaning, and after each successive cleaning round. The arsenic peak at ~197.1 nm displays reduction of arsenic from ~ 8.86 µg/cm^2 before cleaning to close to background after four cleaning rounds. A smooth line function has been applied to the data as a guide to the eye.

Figure 14 above demonstrates the effect of each laser cleaning round for eductor tube test piece ET-10A. LIBS analysis of the test piece prior to cleaning showed ~8.86 µg/cm^2 arsenic associated with the oxide layer. After the first round of laser cleaning the surface arsenic concentration has been reduced to approximately 1.4 µg/cm^2, then to ~ 0.6 µg/cm^2 with the second round, then to ~ 0.2 µg/cm^2 after the third round, with the fourth round removing arsenic to below detection limit.

Figure 15 (right) shows before and after laser cleaning photographs of an example eductor tube piece (ET-1A). The bright red/orange oxide is removed during the laser cleaning operation. Test pieces typically appeared as cleaned carbon steel surfaces immediately after

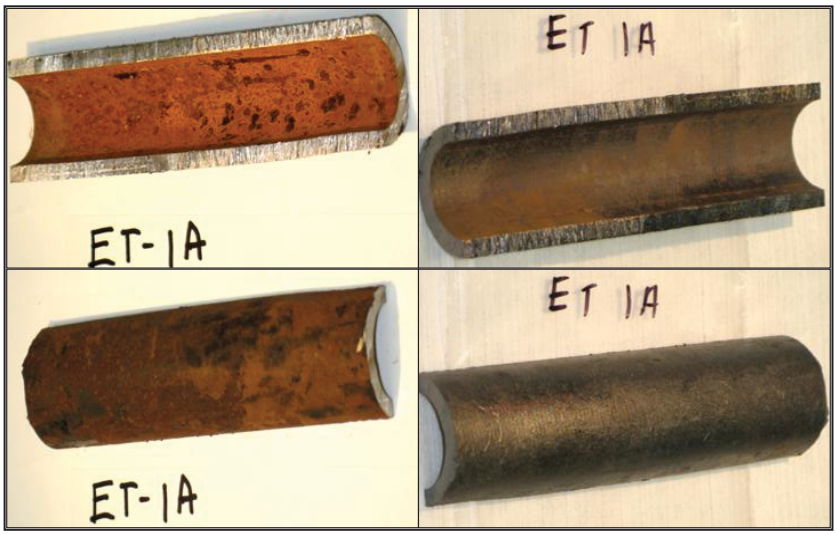

Figure 15. Pre- and post-laser cleaned eductor tube ET-1A.

laser cleaning, but were susceptible to oxidation even when kept in a dessicator. The photographs on the left of Figure 15 (top/bottom), show eductor tube ET-1A inside/outside before laser cleaning. The photographs on the right side (top/bottom), show the inside/outside after laser cleaning. Oxidation seen on laser-cleaned ET-1A inside (upper right) was not present immediately after laser cleaning, and began to appear after about 4 days while sitting in a sealed re-closable sample bag. It was noted that if the cleaned surfaces were not protected (oiled), or kept in an inert atmosphere, then the bare carbon steel would readily begin to rust.

Figure 16. Pre- and post-laser cleaned eductor tube ET-14B.

Figure 16 (right) shows before and after laser cleaning photographs of eductor tube specimen ET-14B. This series of photographs demonstrates surface texture of the cleaned tubes after several rounds of laser cleaning. Surface imperfections, present on test pieces before cleaning but occluded by the oxide layer, become evident after the oxide has been removed.

Data in Table 2 above shows that eductor tube arsenic concentrations are highly variable from tube to tube and from one location on a tube to another location on the same tube. The degree of inhomogeneity was anticipated based on results of a previous study [22]. Eductor tubes arose from ton containers, but the history of each tube, which ton container it came from, and the history of that ton container are lost. Eductor tubes were also shipped un-segregated in the same shipping container which promoted cross-contamination. Ten of the fourteen test pieces shown in Table 2 are opposing half-pieces (e.g., ET-1A and ET-1B, etc). Differences in arsenic concentration from one half-piece to the other half-piece can vary by as much as ~72% (e.g., 5A vs. 5B). Because surface contaminant heterogeneity is so high, the size of the surface sample population acquired via LIBS must also be correspondingly high; otherwise surface analysis techniques may inadvertently "miss" seeing contaminant if the sample population is too low or the area sampled is too small. The LIBS laser is focused to a point that affects an area slightly less than ~1 mm in diameter. If twenty-five single LIBS shots are acquired from different locations on a surface, the total area sampled by LIBS is ~0.2 cm^2. Whereas twenty-five LIBS shots may be a sufficient sample size for a homogeneous surface like the standardized coupons, a larger sample population may be required for the degree of heterogeneity present on the eductor tubes. The high degree of surface heterogeneity combined with acquisition of LIBS shots from a relatively small surface can pose some problems as will be displayed below in Table 3.

Table 3. Results for Selected Acid-Etched Eductor Tubes. LIBS Before, LIBS After, and Acid Etch.

Sample	Area (cm^2)	LIBS Before Laser Cleaning Arsenic ($\mu g/cm^2$)	LIBS After Laser Cleaning Arsenic ($\mu g/cm^2$)	Acid Etch Arsenic ($\mu g/cm^2$)	Exposure Cycles
ET-1B etch sample	185.2	0.82	BDL	0.03	1
ET-2B etch sample	208.8	1.05	BDL	0.37	1
ET-5B etch sample	190.0	1.89	BDL	0.38	1
ET-6B etch sample	182.3	6.16	BDL	0.61	2
ET-13B etch sample	217.0	5.03	BDL	0.10	2
ET-14B etch sample	201.5	3.03	BDL	0.08	1
ET-9B chemically cleaned and then etched**	183.0	N/A	N/A	0.02	N/A

Table 3 gives results for selected post-laser cleaning, post-LIBS analyzed eductor tubes. Tubes were selected and immersed in a 30% aqua regia acid etch. The table provides data for the total surface area of the test piece and the ICP-MS analysis result from the etchate solution. As part of the post-cleaning analysis activities, selected tubes that had already been analyzed via LIBS were weighed and then placed into 30% aqua regia and etched. The tubes were removed from the etch solution after ~5 minutes, rinsed with nanopure water, and the etchate and rinsate were combined into a volumetric flask for standardized dilution. Diluted samples were filtered to 0.45 µm and a portion collected for ICP-MS analysis. Since the etching process is full immersion, the complete surface area of the test piece is exposed to the etching solution. The etching process results in a more thorough "sampling" of the surface than any other technique known. Sample ET-9B (denoted by **) is a half-piece of eductor tube that had been chemically etched and rinsed using an exhaustive process which removes all surface contaminants; leaving behind only the basis metal. ET-9B serves as the background sample for comparison of arsenic that is naturally occurring in the ton container basis metal. By comparing LIBS data from Table 2 to data found in Table 3 we see that detectable arsenic remained on the surfaces of the laser cleaned eductor tubes in some instances. The amount of arsenic remaining was not above the administrative action level, but it was there and detectable nonetheless. In the cases of ET-2B, ET-5B, and ET-6B the arsenic remaining on the sample was within the LIBS detection limit. This is not an issue of "non-detect" or "insensitivity" on the part of the LIBS. Rather, this is clearly an "administrative" issue; an indication of a LIBS sample population and surface sampling spatial distribution scheme that obviously failed to include enough samples from an affected area on the eductor tube that still had detectable arsenic. Determining the proper number of samples and proper sample spatial distribution on real-world surfaces is often an iterative process. Eductor tube pieces were irregularly shaped and had highly heterogeneous spatial distribution of analyte. Use of the sampling chamber improved the quality of the LIBS measurements tremendously, but the sample chamber configuration inadvertently introduced spatial constraints related to which areas of the sample could be easily analyzed without opening the sample compartment door while the LIBS laser was running. For the eductor tube samples, the analyst can minimize the issue of potentially "overlooking analyte" remaining on the surface after laser cleaning by a) increasing the number of LIBS shots, b) dispersing LIBS shots over a larger total surface area of the sample, c) employ a four-axis sample stage or a sampling configuration that allows access to all parts of the sample, and d) analyzing single shot spectra as opposed to composite data. The LIBS sampling scheme that was employed acquired 25 single shots and then made a single composite spectrum. On highly heterogeneous surfaces where sample distribution is also highly heterogeneous a composite spectrum could artificially under-report analyte present on the surface. If a shot were acquired from an area that contained significant arsenic, followed by a shot from an area that was clean, then in the "composite" scheme the resulting spectrum is an average of the two individual spectra, which would result in under-reporting the actual amount of arsenic. By analyzing single-shot spectra, the actual amount of arsenic present in the beam sampling area is accurately reflected. The bulk of the work analyzing spectra then falls to the analyst and the spectral analysis software.

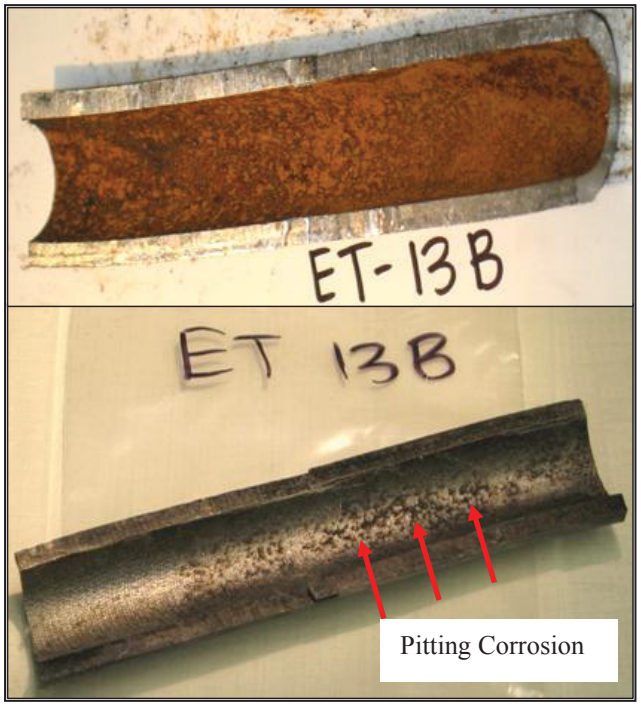

Figure 17. Pictures of pre- and post-laser cleaned eductor tube piece ET-13B. The dark areas on the cleaned piece (bottom) are areas of pitting corrosion.

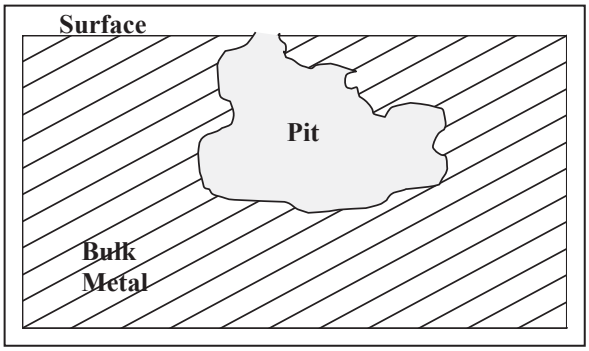

Figure 18. Diagram of a cross-section of advanced localized corrosion forming a pit into the basis metal.

Another contributor to finding analyte in the acid etch samples was the presence of pitting corrosion on the eductor tubes. Figure 17 (above) shows eductor tube ET-13B before (top), and after (bottom), laser cleaning. After the surface oxide had been removed by the laser some tube pieces showed dark splotches. Upon closer examination it was found those dark areas were areas of advanced pitting corrosion. Pitting corrosion is localized corrosion that creates small holes in a metal. Pinholes are often difficult to notice and are obscured by corrosion products. Whereas the pinhole can be small, the rate of corrosion can be quite advanced leading to formation of deep pits and crevices beneath the surface (Figure 18). Contaminants permeate into the pits if the surface is exposed to liquids, creating deep pockets of concentrated contaminant. Such pits can pose a challenge not only for detection via LIBS, but also the cleaning laser because the spot size of the cleaning laser is on the order of ~300 microns. If the laser operator does not happen to see areas of pitting corrosion, then the cleaning laser beam can be passed over the area too rapidly during the initial laser cleaning. The narrow mouth of the pinhole could occlude the cleaning laser beam, leaving most of the contents of the pit untouched. If the follow-on LIBS analysis does not happen to hit one of the narrow, deep pockets, then contaminant could be under-reported. Acid etching of the surface is a full-immersion process which cleans out all pits and crevices. The observed presence of pits, along with the appearance of analyte in the acid etch samples points directly to pits on the eductor tubes that were not properly cleaned during laser surface cleaning, went unnoticed in follow-on LIBS surface analysis, and did not become apparent until after the fact when arsenic began showing up in the acid etched samples. Areas of pitting corrosion which were noted and caught by the cleaning laser operator were subject to more intense localized cleaning. The cleaning laser can clean the pits, and the LIBS can successfully analyze pitted areas, but the process employed in these tests was only as good as the cleaning laser operator's visual acuity and experience.

4. CONCLUSIONS

Real world surfaces, in the form of fourteen different eductor tube test pieces, were analyzed and then laser cleaned. LIBS analysis of eductor tube surfaces before laser cleaning showed some surfaces to be highly contaminated. LIBS analysis after laser cleaning demonstrated the cleaning laser to be capable of effectively removing real world arsenic and mercury surface contaminants. Some eductor tubes required several rounds of laser illumination; others required only a single session. All tubes were cleaned of arsenic to below the administrative control level, and post-cleaning analysis using acid etching demonstrated that fact. Valuable lessons were learned about laser cleaning surfaces and how to more effectively employ a laser cleaner. How to identify and clean areas of pitting corrosion, and the limitations inherent to relying on visual/audible stimuli have shaped and influenced our thoughts for improving the cleaning and analysis process. A valuable lesson was learned in operating the LIBS spectrometer on highly heterogeneous surfaces. When analyzing such surfaces the analyst should consider acquiring a larger number of shots dispersed over a larger sampling area. The acquisition mode should be single shot analysis as opposed to making a composite of spectra. Configurational constraints which may limit the area available for analysis on surfaces and parts should be considered and steps should be taken to ensure adequate sampling that is representative of occluded areas. Such issues are "administrative" in nature and very correctable. Lessons learned in the acquisition of data from real world samples do not reflect any limitation on the part of LIBS or the cleaning laser. LIBS was demonstrated as a sensitive and useful field-deployable analytical technique capable of detecting arsenic at levels that are an order magnitude below the administrative action level (1 $\mu g/cm^2$). New instrumentation being tested at Applied Photonics Ltd. shows a LIBS detection limit for arsenic that is nearly two orders magnitude below the administrative control limit on standardized coupons. The key to successfully laser cleaning a surface is to use LIBS to guide the cleaning effort on-the-spot.

5. FUTURE DIRECTIONS

It is envisioned that a single, laser-based, automated cleaning and analysis platform is achievable. Terminal optics are available from the cleaning laser manufacturer (Figure 19) which interface with multi-axis, articulating arm robots. Automation of the laser cleaning component will lead to application of the minimum amount of laser power to the surface needed to achieve "clean" as determined by the LIBS. Judicious use of laser power will minimize unnecessary ablation markings, reduce operator-related over-illumination of the surface, and will aid in reducing thermal oxidation of the surface. Mounting of the laser end-effector on a stepper-motor-controlled articulating platform will allow optimal focal distance positioning, standardized translation rate over the surface, and minimal treatment overlap. Addition of an

inert sweep gas (e.g., N_2) through the end-effector during laser cleaning would aid in minimizing thermal oxidation. Use of diffuse reflectance spectroscopy to assess surface oxide species and surface quality before and after laser illumination would allow additional direct feedback control of laser power to prevent over-illumination of the surface. Robotic operation of laser cleaning would provide a much more precise and methodical approach to efficient removal of surface contaminants.

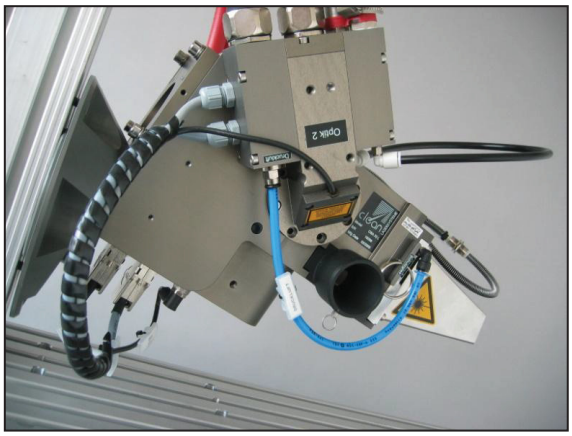

Figure 19. OSA 70 optic from Adapt-Laser. This end-effector is designed for robotic applications. Photo courtesy of Adapt-Laser.

Near-real-time LIBS analysis of surfaces with the LIBS unit mounted on an $x - y - z$ stepper-motor platform would allow surface contaminant mapping and much finer control, almost prescription control, of where laser cleaning efforts would need to be concentrated. A LIBS spectrometer equipped with a higher resolution spectrograph (e.g., Catalina Scientific EMU-65) will allow for easier discrimination between analyte signal and background interference arising from Fe, and Ni lines (carbon steels, stainless steels). Equipping the EMU-65 spectrograph with a UV-sensitive, low-light camera (e.g., EMCCD) will allow for higher signal throughput and arsenic/mercury detection limits to reach 2 – 3 orders magnitude below current US Army administrative control levels. Figure 20 shows a spectrograph of arsenic on steel using an EMU-65 spectrograph equipped with an EMCCD camera.

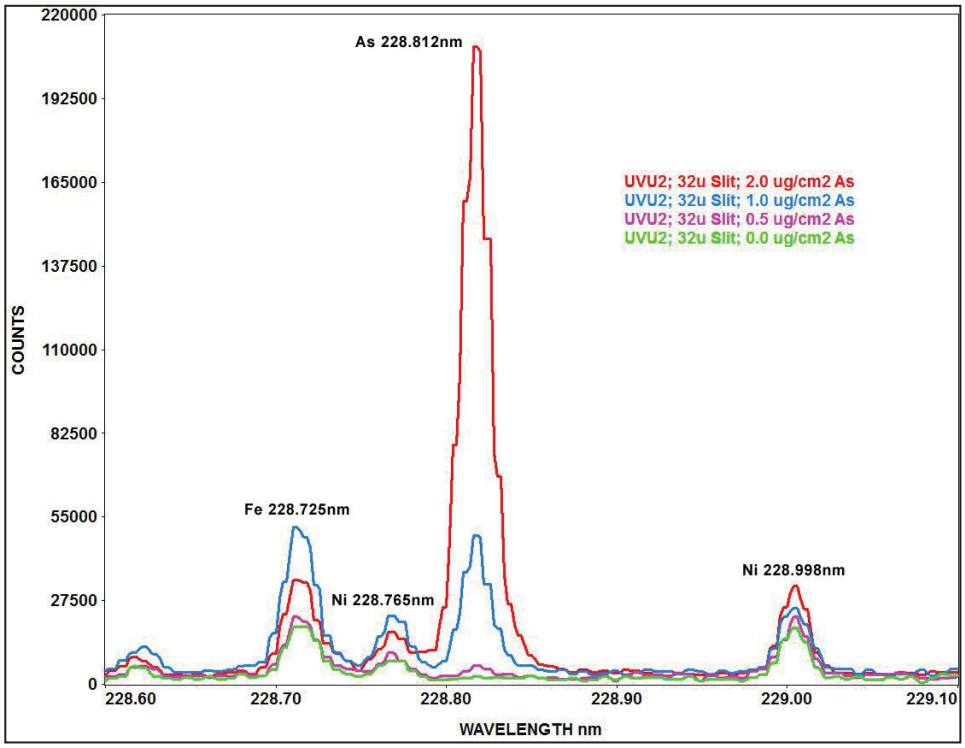

Figure 20. Spectrograph of arsenic on steel using a Catalina Scientific Instruments LLC, (Tucson, AZ) EMU-65 equipped with an EMCCD camera. Spectra courtesy of Catalina Scientific Instruments.

Also of interest is continued pursuit of a real-time LIBS technique which uses the plasma light generated from the cleaning laser to generate LIBS spectra. As the cleaning laser progresses over the surface, plasma is created. It was envisioned that plasma light could be captured by a spectrograph and used to generate real-time LIBS spectra of the analyte on the surface being cleaned. To investigate that phenomenon the cleaning laser used in the current study was aimed at a contaminated eductor tube (Figure 21). A collection lens and fiber-optic lead was also aimed at the surface to capture plasma light generated by the cleaning laser. The outcome of that experiment demonstrated that although existing equipment could not be used, it would not be impossible to configure a system that could work. Such a system would employ a shutter to gate plasma light going to the spectrometer. The shutter and the LIBS camera would trigger off the Q-switch of the laser. The cleaning laser may also have to be configured with a "burst mode" to focus and generate enough plasma light in a single pulse to be useful for LIBS spectra. The collection optic which captured the plasma light would need to be large and efficient in order to capture enough light. Investigation and further development are currently under consideration.

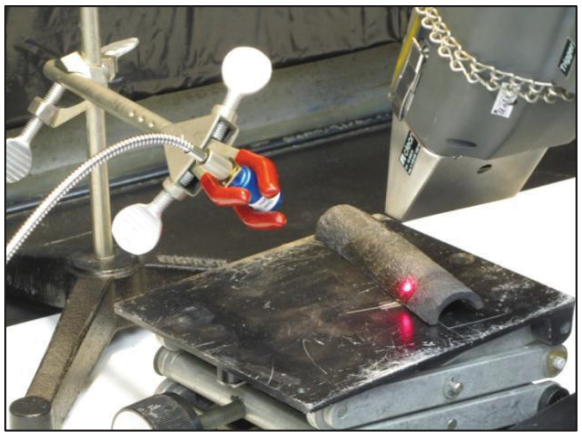

Figure 21. Experiment to try to capture plasma light from the cleaning laser.

A combined cleaning/analysis robotic platform is currently under construction and will be tested for use cleaning an Explosives Destruction System (EDS) vessel. The EDS is a device that is used in the demilitarization of chemical munitions. As part of a demilitarization campaign the vessel frequently undergoes cleaning. A cleaning/analysis robot (conceptual design seen below in Figure 22) will be constructed which includes end-effectors for the cleaning component, and the LIBS analysis component. Tests are expected to begin in the Spring of 2014.

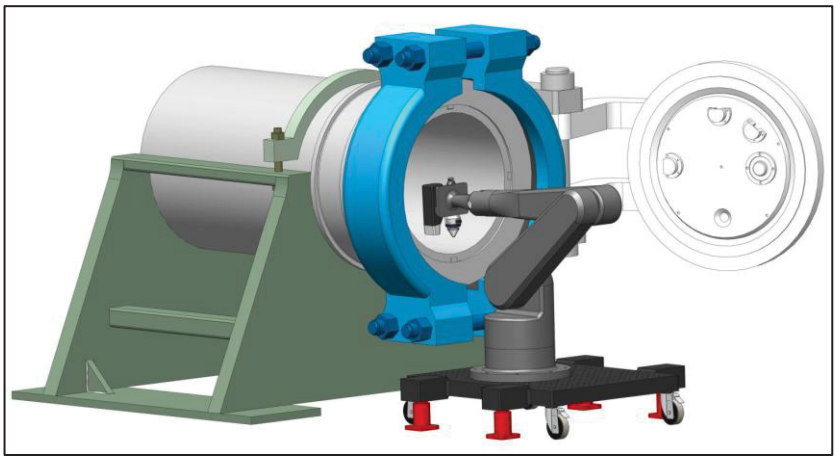

Figure 22. Conceptual model of a single robotic platform comprised of a 6-axis articulating arm, an end-effector for laser cleaning, and a high-resolution, field-portable LIBS spectrometer mounted on the end-effector.

ACKNOWLEDGEMENTS

This program was funded by the US Army Project Manager – Non Stockpile Chemical Materiel and performed under DOE Idaho Operations Office Contract DE-AC07-05ID14517. The authors would also like to thank Burt and Wendy Beardsley of Catalina Scientific Instruments, LLC for the arsenic spectra found in Figure 20. INL/CON-13-28860.

REFERENCES

[1] Barletta, M, Gisario, A., and Tagliaferri, V., "An application of a high power diode laser to remove oxides on AISI 316L stainless steel," Int. J. Materials and Product Technology 32(1), 71-91 (2008).
[2] Bloisia,F., Baroneb, A.C., Vicari, L., "Dry laser cleaning of mechanically thin films," Applied Surface Science 238, 121–124 (2004).
[3] Zhang, A., Wang, Y., Cheng, P., and Yao, Y.L., "Effect of pulsing parameters on laser ablative cleaning of copper oxides," J. Applied Phys. 99, 064902-1 – 064902-11 (2006).
[4] Zapka, W., Ziemlich, W., "Efficient pulsed laser removal of 0.2 pm sized particles from a solid surface," Appl. Phys. Lett. 58 (20), 2217-2219 (1991).
[5] Guo, H., Martukanitz, R., DebRoy, T., "Laser assisted cleaning of oxide films on SUS409 stainless steel," J. Laser Applications 16(4), 236-244 (2004).
[6] Allen, S.D., Miller, A.S., Lee, S.J., "Laser assisted particle removal 'dry' cleaning of critical surfaces," Materials Science and Engineering B49, 85-88 (1997).
[7] Siano, S., Agresti, J., Cacciari, I., Ciofini, D., Mascalchi, M., Osticioli, I., Mencaglia, A.A., "Laser cleaning in conservation of stone, metal, and painted artifacts: state of the art and new insights on the use of the Nd:YAG lasers," Appl. Phys. A 106, 419–446 (2012).
[8] Tam, A.C., Leung, W.P., Zapka, W., and Ziemlich, W., "Laser-cleaning techniques for removal of surface particulates," J. Appl. Phys. 71 (7), 3515-3523 (1992).
[9] Veiko, V.P., Mutin, T.Y., Smirnov, V.N., and Shakhno E.A., "Laser decontamination of radioactive nuclides polluted surfaces," Laser Physics 21(3), 608–613 (2011).
[10] Lee, J.M., and Watkins, K.G., "Laser removal of oxides and particles from copper surfaces for microelectronic fabrication," Optics Express 7(2), 68-76 (2000).
[11] Feng, Y., Liu, Z., Vilar, R., Yi, X.-S., "Laser surface cleaning of organic contaminants," Applied Surface Science 150, 131–136 (1999).
[12] Daurelio, G., Chita, G., Cinquepalmi, M., "Laser surface cleaning, de-rusting, de-painting and de-oxidizing," Appl. Phys. A 69, S543–S546 (1999).
[13] Nilaya, J.P., Raote, P., Kumar, A., Biswas, D.J., "Laser-assisted decontamination—A wavelength dependent study," Applied Surface Science 254, 7377–7380 (2008).
[14] Pouli, P., Oujja, M., Castillejo, M., "Practical issues in laser cleaning of stone and painted artefacts: optimisation procedures and side effects," Appl. Phys. A 106, 447–464 (2012).
[15] Psyllaki, P., Oltra, R., "Preliminary study on the laser cleaning of stainless steels after high temperature oxidation," Materials Science and Engineering A282, 145–152 (2000).
[16] Koh, Y.S., Powell, J., Kaplan, A.F.H., "Removal of layers of corrosion from steel surfaces: A qualitative comparison of laser methods and mechanical techniques," J. Laser Applications 19(2), 99-106 (2007).
[17] Kameo, Y., Nakashima, M., , and Hirabayashi, T., "Removal of metal-oxide layers formed on stainless and carbon steel surfaces by excimer laser irradiation in various atmospheres," Nuclear Technology 137, 139-146 (2002).
[18] Kane, D.M., Fernandes, A.J., Mildren, R.P., "Optical microscopy imaging and image-analysis issues in laser cleaning," Appl. Phys. A 77, 847–853 (2003).
[19] Bregar, V.B., Mozina, J., "Optoacoustic analysis of the laser-cleaning process," Applied Surface Science 185, 277-288 (2002).
[20] Jezersek, M., Milanic,, M., Babnik, A., Mozina, J., "Real-time optodynamic monitoring of pulsed laser decoating rate," Ultrasonics 42, 37–41 (2004).
[21] Fox, R.V., Groenewold, G.S., "Evaluation of selected inorganic CWM byproducts on ton container eductor tubes and steel coupons, and implications for laser cleaning," Idaho National Laboratory INL/LTD-12-24808, (2012).
[22] Groenewold,G.S., Avci, R., Fox, R.V., Deliorman, M., Suo, Z., and Kellerman, L., "Characterization of arsenic contamination on rust from ton containers," Ind. Eng. Chem. Res. 52, 1396−1404 (2013).